A new method for examining maritime mobility of direct crossings with contrary prevailing winds in the Mediterranean during antiquity

Article *in* Journal of Archaeological Science · May 2021

DOI: 10.1016/j.jas.2021.105369

CITATIONS
5

READS
328

3 authors:

David Gal
University of Haifa
3 PUBLICATIONS **6** CITATIONS
SEE PROFILE

Hadas Saaroni
Tel Aviv University
106 PUBLICATIONS **4,306** CITATIONS
SEE PROFILE

Deborah Cvikel
University of Haifa
91 PUBLICATIONS **570** CITATIONS
SEE PROFILE

Journal of Archaeological Science 129 (2021) 105369

Contents lists available at ScienceDirect

Journal of Archaeological Science

journal homepage: http://www.elsevier.com/locate/jas

A new method for examining maritime mobility of direct crossings with contrary prevailing winds in the Mediterranean during antiquity

David Gal [a,*], Hadas Saaroni [b], Deborah Cvikel [a]

[a] Department of Maritime Civilizations and the Leon Recanati Institute for Maritime Studies, University of Haifa, Haifa, 3498838, Israel
[b] Department of Geography and the Human Environment, Porter School of the Environment and Earth Sciences, Tel Aviv University, 6997801, Ramat Aviv, Tel Aviv, Israel

ARTICLE INFO

Keywords:
Ancient sailing routes
Experimental archaeology
Graeco-Roman period
Maritime connectivity
Simulated sailing
Weather-routing

ABSTRACT

The use of detailed meteorological data with sailing software, in conjunction with sailing the *Ma'agan Mikhael II* replica ship, has engendered the development of a method for examining maritime mobility of single-masted square sail Mediterranean merchantmen in the Graeco-Roman period, with the initial objective of mapping direct, open sea, return sailing routes from the Levant that a priori lie contrary to the prevailing wind. Many quantitative works have used averaged winds as input, and evaluated sailing passages based on climatological averages, losing information on the intra- and inter-diurnal variability of the winds. Thus their sole measure of mobility has been a representation of sailing speed on direct crossings. Moreover, these studies have not considered the difference between physical and practical mobility, the latter driven by human factors. For instance, the choice of whether to sail, or wait for better conditions. The proposed method uses climatological resources at high spatial and temporal resolutions, with the premise that using high-resolution data reveals the recurring wind variabilities and patterns that are key to mobility, especially on routes lying contrary to the prevailing winds. The method generated a large set of over 5400 simulated sailing outcomes for each route segment, permitting well-established statistical analysis. Inclusion of criteria-based human factors of the mariners of the period provides a measure of mobility, representing not only sailing speed, but also waiting time, and the probability of conducting a feasible passage at a given time of the year. This new method provides deeper insight into maritime mobility and the understanding of seafaring in the Mediterranean, and is applicable to numerous scenarios, providing a practical and improved measure of maritime mobility.

1. Scientific background

Maritime mobility is the facilitator of maritime connectivity, and can be considered as a foundation block in Mediterranean history (Broodbank, 2013; Horden and Purcell, 2000). However, the archaeological and literary records provide little insight into seafaring practices and capabilities in the Graeco-Roman period. This has led scholarship to derive understandings of ancient maritime mobility from three factors affecting it: (1) Ship technology, expressed by sailing performance, and in particular by windward capability; (2) Environmental conditions, primarily wind and sea current regimes; and (3) The human factor of the seafarers executing the mobility, whose prerogative was to sail only in conditions that they considered reasonable and safe. Applying the human factor differentiates between pure technological evaluation of maritime mobility, namely, what the ships were physically capable of doing, and practical evaluation, i.e., what the mariners were reasonably able to do. Exclusion of the human factor precludes the possibility of assessing measures of practical mobility, such as factoring the time spent waiting for favourable winds.

1.1. Difficulties in examining maritime mobility

The primary drawback in the examination of maritime mobility lies in the fact that most quantitative studies have used climatic averages of wind data at extremely low temporal and spatial resolutions, thus losing information on the significant variabilities of Mediterranean winds that affect mobility (Section 1.3). One exception is a recent study by Warnking (2016) who recognised the limitations of using averaged winds, and conducted a small set of simulations on predominantly downwind routes, using a single six-month span of wind data at a 12-h

* Corresponding author.
E-mail addresses: dgal11@campus.haifa.ac.il (D. Gal), saaroni@tauex.tau.ac.il (H. Saaroni), dcvikel@research.haifa.ac.il (D. Cvikel).

https://doi.org/10.1016/j.jas.2021.105369
Received 22 November 2020; Received in revised form 1 March 2021; Accepted 8 March 2021
Available online 16 March 2021

temporal resolution. However, Warnking's examination focused on sailing speed alone, and did not include human factors. A study by Davies and Bickler (2013), tailored to the Pacific region, is recognised to have used non-averaged wind inputs and to have included human factors.

The second obstacle in measuring maritime mobility is the ongoing discord regarding upwind sailing performance of sailing ships of the period. Scholarly opinions span from ships being considered effectively omnidirectional, with the ability to advance towards a windward destination at a windward velocity made good (VMG) of 2 knots (Casson, 1995; Whitewright, 2011), to understandings that the period loose-footed square sail rig was clearly non-omnidirectional, and could not sail closer than 90° to the wind (McGrail, 2004; Palmer, 2009; Pryor, 1988). A middle-of-the-road opinion suggests that, although ships had a marginal upwind capability, in practical terms mariners did not conduct upwind passages (Murray, 1993; Whitewright, 2018). The discord is fuelled by the fact that there are virtually no scientifically measured data from previous replica ships representing period merchant ships (Cariolou, 1997; Katzev, 1990). Experimental archaeology inputs from sailings of *Ma'agan Mikhael II* replica have contributed valuable insight into the seafaring issues of upwind sailing.

The third drawback, common to all quantitative studies based on GIS cost surface analysis (Alberti, 2018; Leidwanger, 2013; Safadi and Sturt, 2019; Scheidel et al., 2012), is that they only attempted to measure theoretical mobility, based on averaged winds and ship performance. These studies did not address practical mobility, considering the human factors described above. This is in contrast to qualitative studies, which provide ample suggestions as to the conditions in which mariners would or would not sail (McGrail, 2004; Morton, 2001; Pryor, 1988).

1.2. Modern weather vs ancient weather

The possibility of asserting that present weather conditions represent ancient times is key to any study attempting to understand ancient sailing routes based on modern wind data. This question has been raised by many scholars of ancient seafaring, all of whom have concluded that present climate data can be used to represent ancient weather in the Mediterranean (Beresford, 2013; McGrail, 2004; Murray, 1987; Pryor, 1988, 2014). Murray (1987), in his seminal work, investigated the characteristics of Mediterranean winds as described in the historical and archaeological records. He showed, with high confidence, that ancient winds in the Aegean Sea and the eastern Mediterranean were equivalent to the present-day wind regime.

Unfortunately, palaeoclimatological research does not provide direct proxies to give an indication of wind regime; thus indirect proxies are used to indicate that the global atmospheric circulation 3000 years ago is closely equivalent to that of today. More recent research, using alkenone as a paleo bio-indicator for sea surface temperatures (SST) to indicate historic temperatures, has established the corresponding atmospheric circulation, using global circulation models (Lorenz et al., 2006, Figs. 7 and 8; Rimbu et al., 2003, Fig. 4). These studies have indicated that in the last 7000 years there has only been a small change in the Arctic Oscillation (AO) and the North Atlantic Oscillation (NAO) indices, accompanied by a small drop of 1.5 hPa (hectopascal pressure unit = 1 mbar) in the average sea-level pressure (SLP) in the Mediterranean. They concluded that changes in the circulation patterns in the last 3000 years are even smaller. Based on these studies and on identified tele-connections between large-scale atmospheric oscillations and the regional synoptic patterns over the eastern Mediterranean (Ulbrich et al., 2012, sec. 5.2), it is possible to claim that the distribution and occurrence of eastern Mediterranean synoptic patterns have not been changed, and therefore the wind regime has also remained unchanged.

1.3. Variability of Mediterranean winds

The use of wind data at low temporal resolution is most problematic, since it masks the inter- and intra-diurnal[1] variations that are especially large in the Mediterranean region. These variations in the eastern Mediterranean are larger during the winter and the transitional seasons, due to the various synoptic systems prevailing during these times, changing on average every 2–5 days (Alpert et al., 2004a, Fig. 1; Alpert et al., 1989; Saaroni et al., 1998, 1996). Even during the summer season, when the region is dominated by the Persian Trough associated with the persistent Etesian winds (Ziv et al., 2004), inter- and intra-diurnal variations in the wind speed and in weather conditions exist (Harpaz et al., 2014; Saaroni and Ziv, 2000). In addition to the temporal variability of the synoptic patterns, there are meso-scale wind variations, i.e., the breeze circulation at coastal areas and islands, effected also by the nearby topography (Berkovic, 2018, 2016; Klaic et al., 2009; Skibin and Hod, 1979; UK Hydrographic Office, 2005, p. 32; Ulbrich et al., 2012, sec. 5.6.2).

1.4. Typical synoptic patterns in the eastern Mediterranean

An identification and classification of the synoptic patterns of the Levant region, covering also the eastern Mediterranean, was made by Alpert et al. (2004b), and for the Red Sea Trough system by Saaroni et al. (2020). The semi-objective synoptic classification of Alpert et al. defines five synoptic systems, subdivided into 19 sub-types, according to their intensity and location with respect to Israel. The type definition is based on the 12UTC geopotential height, wind and temperature fields at the 1000-hPa level, taken from the NCEP/NCAR re-analysis (Kalnay et al., 1996; Kistler et al., 2001). The systems and types are three types of the Red Sea Trough (RST), three types of the Persian Trough (PT), four types of highs, seven types of Mediterranean Cyclones, or Cyprus Lows, and two types of North African cyclone, or Sharav Lows (SL). For a detailed description of the systems and associated weather conditions over the Levant, see the Appendix of Saaroni et al. (2010).

1.5. Knowledge gaps

Limited understandings of maritime mobility and seafaring issues in antiquity exist, particularly in relation to historical scenarios with routes contrary to prevailing winds. These include, but are not limited to, the westward return routes from the Levant. The knowledge gaps are the compounded results of limited evidence from the literary and archaeological record; the lack of agreement regarding upwind sailing performance; the deficiencies of quantitative methods to examine mobility when using averaged wind data; and their non-inclusion of human factors.

1.6. Objectives

This study proposed a new quantitative method of providing improved measures of maritime mobility for direct sailing passages. The objectives included complementing the physical ship simulation outputs with the introduction of human factors affecting maritime mobility, to obtain measures expressing these human factors, i.e., the time spent waiting for acceptable sailing conditions. The measures of mobility are proposed as improved input data for maritime connectivity analyses. This method is tailored to be adaptable and easily applied to the research of seafaring scenarios.

[1] Intra-diurnal changes occur during each day while inter-diurnal changes occur on time spans of more than one day.

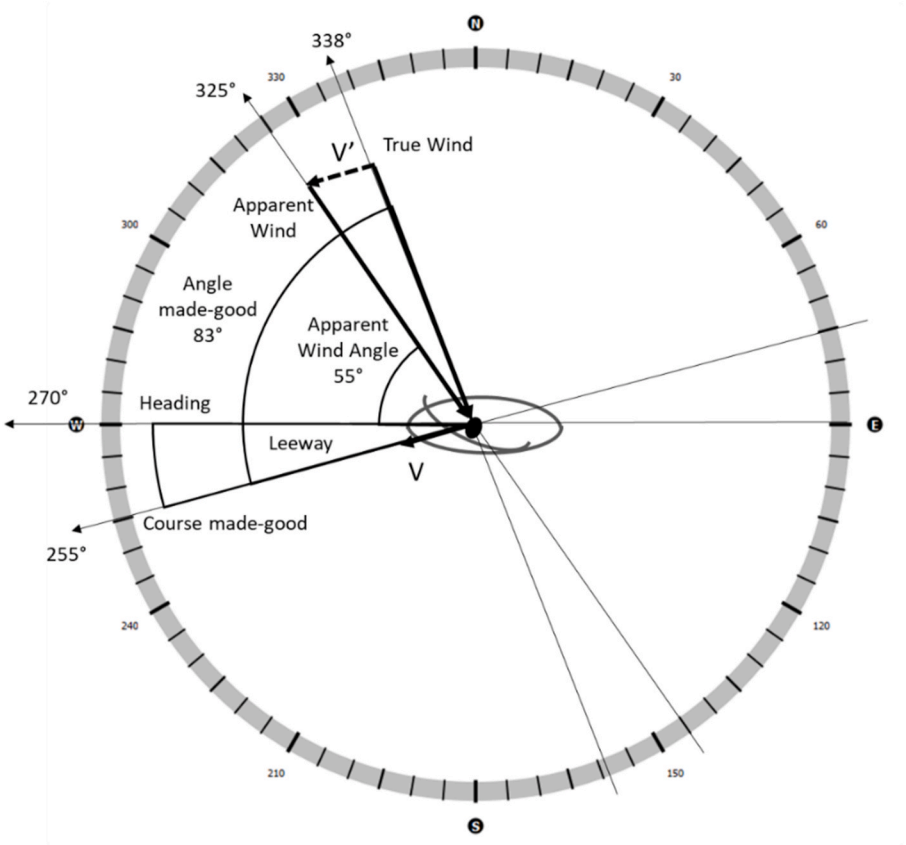

Fig. 1. Example of sailing close-hauled. (Illustration: D. Gal).

2. Method development

2.1. Basic terms and concepts

2.1.1. Definitions

The terms 'passage' and 'route-segment' have been used interchangeably. The term 'voyage' refers to a composite sailing of more than one 'passage'. The term 'velocity made good' (VMG) is used in two contexts: (1) windward VMG is the effective speed vector in the windward direction when sailing close-hauled; (2) passage or voyage VMG is the effective speed of a passage or voyage (calculated as the orthodromic[2] distance divided by the duration). The term 'prevailing wind' is used in an annual context expressing the primary or dominant wind direction which is from the western sector throughout the year unless otherwise explicitly noted.

2.1.2. Sailing close to the wind: A primer

In the following sections references are made to aspects of windward sailing justifying this detour into a brief primer on the process of 'close-hauled' sailing (sailing at an angle as close as possible to the wind) and its associated terms. Fig. 1 illustrates a sailing ship able to maintain a heading of 55° relative to the apparent wind. The apparent wind is the wind that is sensed by the ship and particularly by the sail, and it is measured relative to the ship's heading (Kemp, 1976, p. 30). The apparent wind is the product of the vector of the true wind and the velocity vector of the ship (shown as 'V') which is moving through the air, and therefore inducing an additional airflow vector to that of the wind. When sailing close-hauled, the apparent wind is always ahead of the true wind, and in the given example the difference between the apparent and true winds is 13°, thus the angle of the ship's heading to the true wind is 55° + 13° = 68° (Fig. 1). True wind speed and angle to the ship's heading can be calculated from the readings of apparent wind speed and angle and the velocity of the ship (e.g. Bowditch, 2017, pp. 7, 157).

A period single square sail ship is considered to have had poor lift-to-drag ratios for both the sail and the hull, resulting in significant sideways drift known as leeway (Kemp, 1976, p. 474). Leeway is most evident when sailing close-hauled, and for a period ship it would have been typically 10°–15° or more (Palmer, 2009, pp. 316–7). The angle of leeway needs to be added or subtracted from the ship's heading (depending on the side from which the wind is blowing) to indicate the ship's course made good. In the given example, the effective angle of the ship to the true wind (angle made-good) is heading-to-true-wind plus leeway i.e., 68° + 15° = 83°.

Tacking is when a ship advances to windward, and alternates between sailing close-hauled with the wind on the right (starboard tack) to sailing close-hauled with the wind on the left (port tack) (Kemp, 1976, p. 853). The tacking angle is the angle between the course made good on each tack, and is equal to double the angle made good. In our example: 83° × 2 = 166°. The smaller the tacking angle, the better the windward performance. The example shown in Fig. 1 does not include the drift of sea surface currents.

Care is needed not to use the apparent wind angle alone as an indicator of windward performance. Based on the example presented here, a statement such as "The ship could sail at 55° to the wind", sounds quite optimistic, but as shown in the example, once the differences to the true wind and the leeway are added, we find that the angle made-good to the true wind is only 83°. It is suggested that leeway should neither be ignored nor underestimated. Modern sailing yachts typically suffer only 3–4 degrees of leeway when close-hauled, as their efficient sails generate

[2] Orthodromic distance is the shortest possible distance between two points on a sphere (the earth).

relatively less sideways force, and their keeled hulls very efficiently resist the sideways forces of the sails. In period ships leeway values of 10°–20° would have been the norm (Palmer, 2009, pp. 316–320).

2.2. Data from experimental sailings

The sailing ship *Ma'agan Mikhael II* used in this study (Fig. 2), is a replica of the Ma'agan Mikhael shipwreck, dated to 400 BC (Kahanov and Linder, 2004; Linder and Kahanov, 2003). The construction of the sailing replica, headed by the late professor Yaacov Kahanov, took two years (2014–2016). Its hull reproduced the shell-first construction of the original ship of the ancient shipwrights (Cvikel and Hillman, 2020). The ship was officially launched in March 2017, and so far, has made dozens of voyages along the Israeli coast and a crossing to Cyprus and back. These sailings provided essential information on ancient sailing techniques and ship sailing performance. They also highlighted the potential limits of the ancient mariners in conducting passages in adverse wind conditions.

The *Ma'agan Mikhael II* is equipped with wind sensors, combined with GPS and heading sensors. All sailing data are recorded in a digital voyage recorder. Data accumulated during more than 70 local sailings served to compile a polar diagram, representing the ship's speed over water at specific points of sail and at specific wind speeds (Fig. 3). The polar diagram expresses the relationship between True Wind Speed (TWS) and True Wind Angle (TWA) to the resulting vessel Speed Over Water (SOW). Polar diagrams alone do not provide an indication of windward capability, but only show the close-hauled angle to the true wind that can be maintained.

The polar diagram for the *Ma'agan Mikhael II* (Fig. 3) shows, as a rule of thumb, that the ship's speed will be about 40%–50% of the true wind speed when sailing downwind on a broad reach or a run, and 25% of the true wind speed when close-hauled. For example, a 10-knot true wind at 150° off the bow propels the ship at 4 knots, and the same 10-knot wind at 90° propels the ship at 2.4 knots. The accuracy of the polar diagram was verified by comparing *Ma'agan Mikhael II*'s measured performance on several longer sailing passages of up to 30 h' duration, to the results of weather-routing simulations of the same passages based on the polar diagram. The simulation estimates were within 5% of the actual sailing times.

Determination of angle of the windward course made good must include leeway. For Graeco-Roman merchantmen with single square sail rigs, the close-hauled leeway is estimated to have been in the order of 10°–25°, depending on wind force, waves, hull efficiency and vessel speed. This estimate stems from measurements of the *Ma'agan Mikhael II*, and is supported by findings of other scholarly works. Pomey and Poveda, (2018, p. 54) showed the close-hauled leeway of *Gyptis,* a replica of a 6th century BCE Archaic Greek sewn boat, to be 15°–25°, depending on sea condition, and consider 15° as ideal. Gifford and Gifford, (1998, Fig. 7) estimated the close-hauled leeway of *Sae Wylfing*, a half-scale replica of the Anglo-Saxon Sutton Hoo ship dated 630 CE, to be between 10° and 30°. Palmer (2009, p. 317) indicated a calculated leeway of more than 15° for low efficiency hulls, such as those considered in the present study.

Fig. 2. The Ma'agan Mikhael II replica ship (Photo: A. Yurman).

Sailings of the *Ma'agan Mikhael II* have demonstrated that with a Beaufort force 2 wind and a flat sea, the replica easily maintains a heading 55°–60° to the apparent wind, with speed over ground of 2 knots.[3] This, however, is not as optimistic as it sounds, and equates to maintaining a heading of about 70° to the true wind. With a minimal leeway in these conditions of 15°, the effective angle made-good to the wind, that the vessel is capable of, is, only around 80°–85° (See Section 2.1.2). This provides a mere 0.15 to 0.35 knots of windward VMG, and any windward gains are usually lost in wearing from tack to tack. With typical wind waves of 0.3 m or more, positive windward VMG is no longer obtainable, as hull drag increases rapidly, inducing more leeway. When close-hauled in Beaufort force 3 to 4 conditions with choppy seas, leeway of up to 25° was measured, and windward VMG was only negative. GPS tracks show tacking angles of 190°–200° in these typical Mediterranean open sea conditions.

2.3. Weather data

Weather data used in the simulations were obtained from the ERA5 reanalysis database (Copernicus CDS, 2019; Hersbach, 2016). This source provides gridded reanalysis data at a spatial resolution of 0.25°, equivalent to approximately 27 km and a temporal resolution of 1 h. This high spatial resolution provided more than 7000 data points in the eastern Mediterranean (Fig. 4). The weather data variables used included wind direction (°) and speed (m/s) at 10 m height, SLP (hPa), total cloud cover (%), and wave significant height (m) and mean direction (°). Sea current data was taken from the EU Copernicus Environment Monitoring System repository (EC-Copernicus, 2016). Weather data was extracted for 15 years, from January 2004 to December 2018. This dataset, representing the entire regional sailing environment, included over 930 million sets of data.

2.4. Weather routing simulator

Simulated sailing on the route segments was performed by weather-routing software.[4] We used the qtVlm software (Meltimus, 2017), which calculates isochrones[5] (Fig. 5) spaced 1–3 h apart, and then integrates the most efficient sailing route, i.e., the minimum duration that could have been sailed by the reference ship, departing on a particular date and time for a particular destination, considering the wind and current data existing for the same dates. A single simulated sailing was initiated for each day of the study period for each route segment (a total of 5479 days), departing at 0300 UTC (0500 local solar time). This amounted to more than 135,000 simulated sailings. The departure time of 0300 UTC was chosen to facilitate departing at a time when the land breeze prevails. The temporal resolution of the ERA5 weather data, being 1 h, was reduced prior to simulation to 3 h, to support a more manageable input.

[3] This is similar to the single point report by Katzev (1990, p. 253): "During a 2 h period around sunset *Kyrena II* sailed 50°–60° off the eye of a 2 Beaufort wind, close-hauled, port tack, making over 2 knots speed – evidence of her ability to sail effectively into the wind".

[4] Weather-routing software computes optimal sailing routes for a sailing vessel, given the sailing performance of the vessel, time of departure, and the winds, currents and seas that the sailing vessel will encounter en route (Rabaud, 2016).

[5] Isochrones are lines of equal time. These are calculated for the simulated ship over a range of headings considering the wind speed and direction at every calculated point and time. The isochrones mark where the ship could reach at each step of elapsed time.

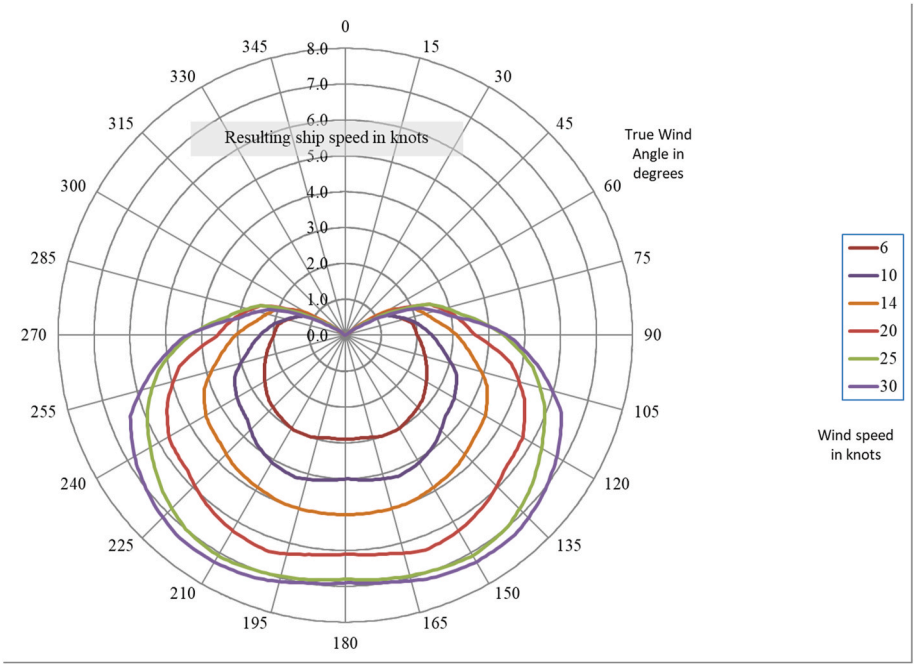

Fig. 3. Polar diagram for the Ma'agan Mikhael II, used in weather-routing simulations. Angles to the wind are in degrees. Wind speed is in knots and indicated by the coloured plots. The intersections of the coloured wind lines with the angle of the wind indicate the ship's speed over the water (Illustration: D. Gal).

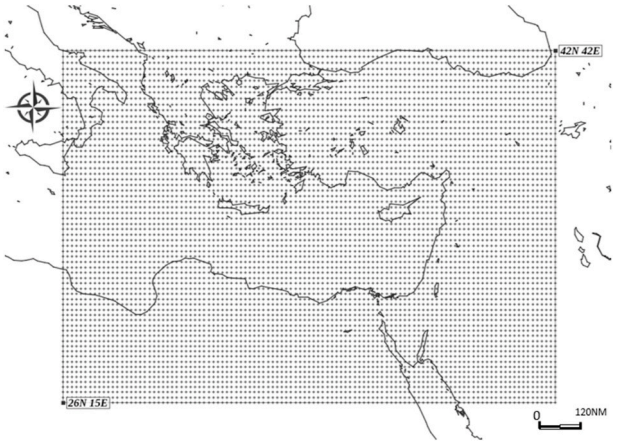

Fig. 4. Spatial coverage (at 0.25° resolution) of the wind and other meteorological data points (7085 points) covering the eastern Mediterranean basin. Map source GSHHS (2004).

This was done after it was verified that this does not affect the quality of the simulations for direct passages.

The simulations modelled the input ship's potential performance for each passage run. Measuring the human factors affecting sailing performance was not an internal component of the simulations, and it was introduced in the analysis of the simulator's output. The output data for each simulated passage included: start date and time; arrival date and time; duration; orthodromic distance; distance sailed; average, maximum and minimum vessel speeds; average, maximum, minimum and average true wind speeds; number of tacks or gybes; beating time[6]; down-wind time; maximum significant wave height encountered; and average cloud cover.

[6] Time spent close-hauled.

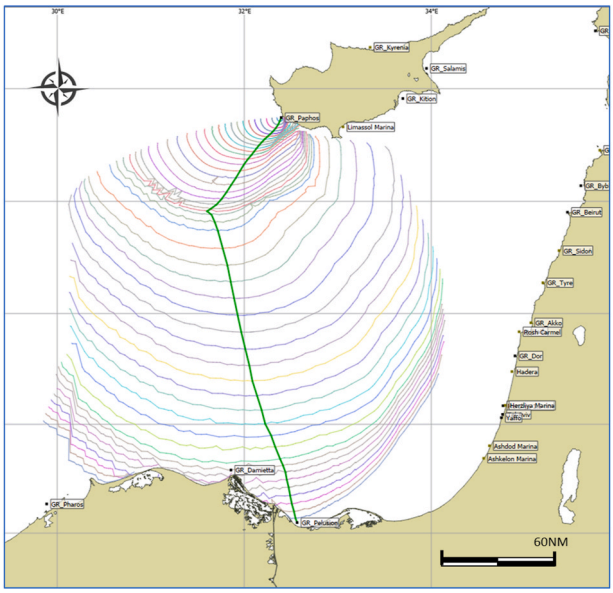

Fig. 5. Illustration of a single weather-routing run from Cyprus to Egypt, showing the isochrones denoting the lines of equal time since departure to which the sailing vessel could have reached at the particular time. The green line shows the resulting shortest time route. (For interpretation of the references to colour in this figure legend, the reader is referred to the Web version of this article.)

2.5. Simulated ship

The simulated ship used in the development of the method to measure maritime mobility, was the *Ma'agan Mikhael II* replica, representing a period merchantman of 20 tons with a single loose-footed square sail (Section 2.2). This particular ship exhibits minimal upwind capability in flat seas and light winds. Considering the possibility that *Ma'agan Mikhael II* may be exhibiting less upwind performance than the average period merchantman, a decision was made to simulate the scholarly

consensus of the middle-of-the-road ship physically capable of limited upwind capability in average sea conditions (Section 1.1).

Consideration was also given to an underlying hypothesis that for upwind passages, the human factors were more limiting than the physical capabilities of the ships, and that mobility may have been driven more by human factors than by the physical degree of ships' upwind capability. This called for simulating a ship technologically capable (i.e. without human factors) of completing simulated passages including upwind passages, and thereafter to determine, based on the detailed summary of the passage parameters, whether it would have been practical for a human crew to conduct these passages. Simulating a ship with no upwind capability would have completely precluded the ability to examine human limits of upwind sailing, as no upwind passages would have been completed.

It was therefore with confidence that the baseline ship for simulation was determined to have the ability to make-good a course of 80° to the true wind in all wind and sea conditions, i.e. sailing about 60° to the apparent wind with about 10° of leeway (Section 2.1.2). The study included comparative simulations for ships with even better upwind performance (i.e. capable of making good 75° and 70° to the true wind) to assess the changes in practical mobility. Comparative simulation of a less efficient ship (i.e. capable of 85°) was not performed, as it was assessed to be marginal once the human factors were found to be more limiting.

The following adjustments to the performance of *Ma'agan Mikhael II* were made to achieve the baseline ship for simulations. The speed envelope of the ship on points of sail other than close-hauled, is mainly a function of sail area to ship displacement, and the replica ship's polar data would have closely represented other period ships, and it was therefore maintained with no changes. The upwind (close-hauled) performance is mainly a function of sail and hull lift-to-drag ratios, and this was the area that was adjusted for the simulated ship to reflect the middle-of-the-road ship (Section 1.1). The simulator derives best windward VMG angles from the polar diagram without considering leeway, but it also provides an indirect method of implementing leeway simulation by setting an override to the angle of best windward VMG. This was set for 80° in all sea conditions, recognising that this is a general parameterisation of leeway that in reality varies with sea and wind conditions.

2.6. Criteria representing human seafaring factors

The weather-routing simulator itself is the 'ultimate sailor'. It makes no navigational errors; it always takes the best routing; it has no limits to its endurance; if necessary, it can change tack hundreds of times a day; it sails in all sea conditions; it always reaches its destination in spite of all difficulties en route; and above all, it has no fear. Simulated departures were never postponed, and passages were never aborted once started. The simulator only simulates the physical ship according to the ship's limitations. Unlike the simulator, ancient mariners would have been selective and applied judgement. They would have chosen not to depart if conditions were unreasonable for them, and they would have aborted sailing passages in which conditions became unreasonable for them en route by returning to point of departure, or by diverting to a nearby safe haven.

The method of introducing the human factor into the examination of mobility was to divide the outcomes of all simulated passages into a set of 'acceptable' passages, that would have been reasonable for a hypothetical ancient mariner to complete, and into a set of 'rejected' passages, i.e., unreasonable to complete. The set of acceptable passages is the dataset from which measures of mobility were derived. The experimental voyages of the *Ma'agan Mikhael II* illuminated seafaring issues, and the ship's skippers were instrumental in defining parameters that would have affected the ancient mariners' abilities to conduct passages.

Two parameters reflecting favourable or unfavourable winds were found to provide a consistent division between what could be considered reasonable passages and those that could be deemed as unreasonable passages. These are the overall passage VMG, and the distance sailed ratio, which is the ratio between passage orthodromic distance, and the actual distance sailed. Passage VMG criterion was set to a minimum of 1.0 knot, and the distance sailed ratio criterion was set to a maximum of 1:1.5 (sailed distance 50% greater than the direct distance). These settings encapsulate the rationale that the main limiting factors for the ancient mariner were: duration at sea, reflected by voyage VMG; the problem of maintaining navigation while on sailing tracks deviating significantly off the direct route, reflected by distance sailed ratio; and situations requiring significant beating towards an upwind destination, reflected by both voyage VMG and distance ratio.

Additional criteria were used to introduce stormy weather into the threshold between 'acceptable' and 'rejected' passages. These are 31 knots (Beaufort 7) for maximum sustained wind speed encountered, and 2.75 m for maximum significant wave height encountered en route. The entire set of criteria was subjected to a sensitivity check.

2.7. Tested routes

The set of routes selected for the development of the method and its initial application suggest the possible direct offshore route segments that the ancient mariners might have sailed when returning from the Levant to Cyprus, Asia Minor or the Aegean (Fig. 6). Route segments lie mainly in directions contrary to the east Mediterranean, year-round, prevailing winds from the north-west. Several segments are in directions that are closely across (about 90°) the prevailing winds, and two segments were selected on a predominantly down-wind direction, for comparison.

In addition to the environment-driven choice of route segments, there is also a historical context. A direct passage from the Levant to Rhodes represents the route taken by Mark the Deacon (*Marcus Diaconus*) in 401 CE (Hill, 1913, pp.42–3, 120); while the route segments along the coast of Anatolia continuing to Crete represent the route taken by Paul on his voyage to Rome (Acts, 27); the passage from Pharos (Alexandria) to Rhodes was a typical winter route for grain supply from Egypt (Demosthenes, 56.30); and the segment from Pharos to west Cyprus represents the initial passage of the Isis (Lucian, Navigium, 7).

3. Method outputs

In the process of running the weather-routing simulations, the software traces the optimal routings solved for each simulated passage on a map. This visual representation illustrates whether the simulated sailings were with favourable winds, or beating against contrary winds. These tracings themselves are a non-quantifiable resource, but they do reflect on the numerical results generated for the same simulated sailings, and serve well to highlight the issue of contrary prevailing winds. Fig. 7 presents the traces of ten consecutive daily sailings on the route segment between Dor and Pharos (Alexandria), which lies predominantly contrary to the prevailing winds. The map for August reflects longer distances sailed due to encountered contrary winds, compared with October, when the distances sailed are much shorter and direct, due to seasonal wind variability with windows of opportunity for favourable winds from the north or north-east.

3.1. Simulated passage summaries

Statistical summaries are extracted for the three sailing parameters that have a dominant bearing on mobility: (1) passage duration (in days); (2) voyage VMG (in knots), which is the effective speed of the passage calculated from the duration and orthodromic distance of the passage; and (3) the distance sailed ratio, which is the ratio of the actual distance sailed to the orthodromic distance of the segment. The summaries are presented separately for each route segment on a monthly basis, and then grouped by the criteria-based division into 'acceptable'

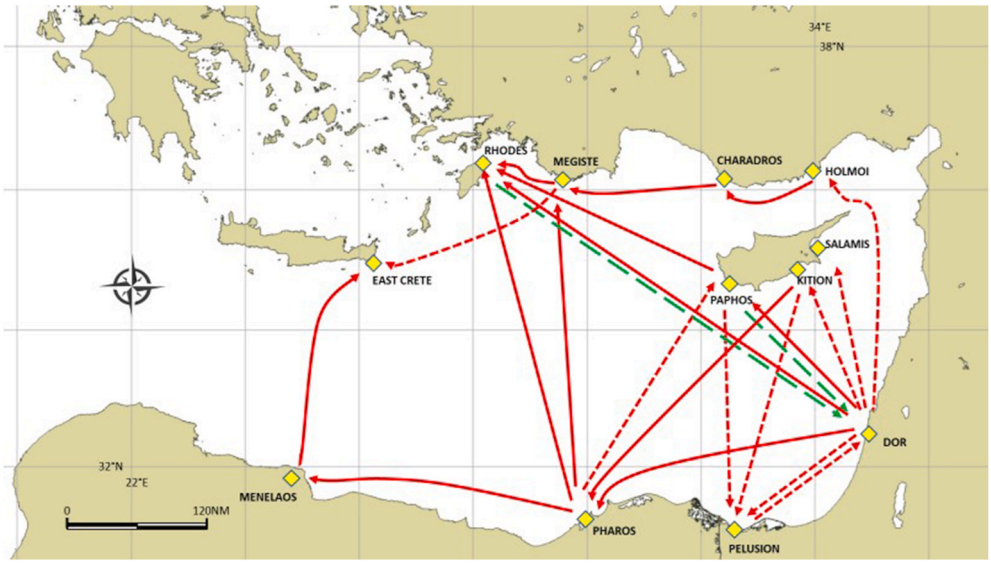

Fig. 6. Route segments examined: Solid red – against prevailing winds; Dashed red – across prevailing winds; Long Dashed green – with prevailing winds. (For interpretation of the references to colour in this figure legend, the reader is referred to the Web version of this article.)

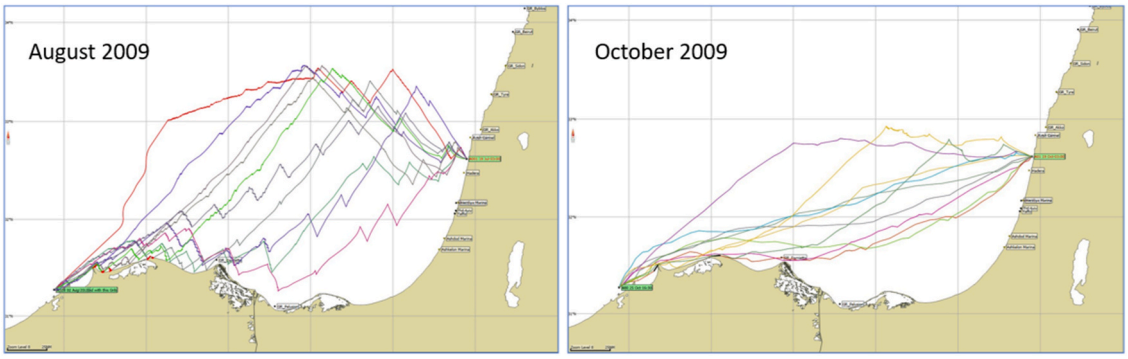

Fig. 7. Simulated routes for ten consecutive days in August and October 2009, illustrating the relative difficulty (beating against contrary winds) of August sailings on the Dor–Pharos (Alexandria) route segment in relation to the relative ease (following winds) in October.

and 'rejected' sailings (see Section 2.6).

The output of sailing parameters for the Dor to Pharos (Alexandria) route (Table 1) throws light on the differences between the August and October sailings shown in Fig. 7. The analysis for all passages shows that in August the average voyage VMG was 0.6 ± 0.1 knots, the average passage duration was 18.6 ± 3.9 days, and the average distance sailed ratio was 3.1 ± 0.6, i.e., the track sailed was over three times the direct distance. Even more extreme results are seen in July. For October, the results for all passages are significantly more optimistic for the mariners: average voyage VMG of 1.7 ± 0.3 knots, average duration of 6.4 ± 1.2 days, and average distance sailed ratio of 1.3 ± 0.2. It is noteworthy that in the set of rejected passages during the winter months, the values of voyage VMG and distance sailed ratio may have values reflecting the 'good' set of criteria. This occurs during depressions when the wind and wave values encountered cause the passages to be rejected.

3.2. Environmental parameter statistics

An additional output of the simulated sailings is that of the environmental conditions encountered by the simulated ships during their passages. The parameters include the average of maximum wind speeds; the average of maximum wave heights; the average wind speed; and the average cloud cover in percent. The example Dor to Pharos route segment (Table 2), is grouped by 'all' sailing passages and by 'acceptable' and 'rejected' sailing passages. Such data provides insight into the sailing conditions that were encountered on a specific route segment in a specific month. For example, the average of the maximum wind speeds shows the highest value of 22.6 knots for all passages in January on the Dor to Pharos route. The highest wind instance in the 15 years of data for this route segment was found to be 37.9 knots (not shown in the table). Similarly, the table shows the average of maximum wave heights being 2.7 m in January. The highest instance of the significant wave height was found to be 7.0 m.

3.3. Measures of potential mobility

The criteria-based division between 'acceptable' and 'rejected' passages (Section 2.6), in itself provides a basis for measuring mobility. A route segment with more opportunities for 'acceptable' passages in a given period has better mobility potential than a route segment with fewer opportunities in the same period. The primary output of the method is therefore a new measure of maritime mobility, namely, the monthly count of daily opportunities that exist to conduct a successful passage on a particular route segment. The complement of this daily count is the number of days that mariners would potentially spend waiting for favourable winds in a particular month. This measure of mobility is supplemented by the monthly average passage VMG and subsequent average duration for the same passage. The following

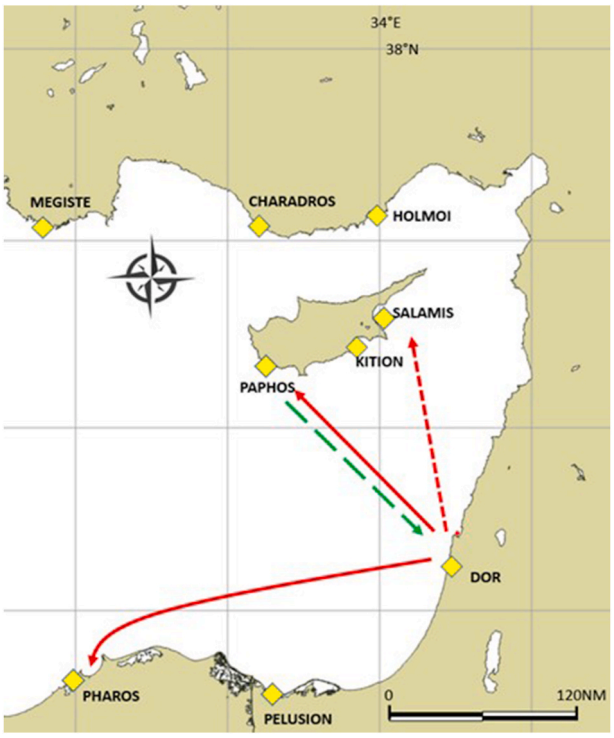

Fig. 8. Example route segments. Solid red: contrary to prevailing winds. Dashed green: with prevailing winds. Dashed red: across prevailing winds. (For interpretation of the references to colour in this figure legend, the reader is referred to the Web version of this article.)

examples present measures of mobility for representative route segments (Fig. 8) that lie contrary to prevailing winds, across prevailing wind, or with the prevailing winds.

Measures of potential mobility are shown in Figs. 9–12, each presenting: the average count of departure days per month having an opportunity to conduct an 'acceptable' passage (red bars together with error bars indicating plus and minus one standard deviation); passage VMG (blue bars); and passage duration (orange bars).

The Dor to Pharos segment (Fig. 9) represents a route segment that is contrary to the prevailing winds, and it shows peaks of opportunities in March–April and in October–November. These peaks are indicative of the occurrences of the RST, associated with north-easterly winds in these months, especially near the coasts of the Levant region (Saaroni et al, 1998, 2020; Tsvieli and Zangvil, 2005).

The passage from Dor to Paphos in the west of Cyprus (Fig. 10), provides another example for a route segment that is contrary to the prevailing winds. It indicates a very low number of opportunities to complete a reasonable voyage during the warm season, from the beginning of May and up to the end of September. The best opportunities for exploiting favourable winds occur during the winter months, November to the end of February, having between 15 to over 20 days a month with passage opportunities.

The mobility analysis for a route segment at right angles to the prevailing winds is shown for the passage from Dor to Salamis in eastern Cyprus (Fig. 11). These results illuminate the unique opportunities for conducting year-round voyages on both the outward and return passages, when winds that are mainly on the beam, i.e., perpendicular in both directions. This is in contrast with routes where outward passages are conducted downwind, causing the return passages to be confronted with the problem of contrary winds. The somewhat reduced mobility shown for September to December is indicative of the prevailing seasonal RST with its north-easterly winds.

The final example of the method's output of mobility is for a route segment that lies with the direction of the prevailing winds, Paphos to Dor (Fig. 12). Note the feasibility of passage opportunities in almost all summer days and in the transitional seasons, showing in this downwind example the higher passage VMG values. The slight reduction in passage opportunities during the winter months is due to days with storm systems, and not due to contrary winds. The criterion of 2.75 m maximum significant height waves was encountered on 22 days per year on this route segment. The criterion of 31 knots maximum sustained wind speed was encountered on 2.2 days per year.

3.4. Relation to synoptic patterns

The database of daily sailing attempts created by the method is linked with a database of daily synoptic patterns that exist for the same dates for the Levant region (see Section 1.4), providing the opportunity of analysing relations between specific synoptic patterns and mobility. This, in turn, provides insight into the ancient mariners' abilities to judge good sailing opportunities based on the combination of time-of-the-year and typical weather patterns.

Table 1
Dor to Pharos, as an example of summarised sailing parameters.

Dor–Pharos Voyage VMG in knots		Jan	Feb	Mar	Apr	May	Jun	Jul	Aug	Sep	Oct	Nov	Dec
All passages	Average	1.6	1.7	1.9	1.8	1.3	0.7	0.4	0.6	1.2	1.7	2.0	1.6
	Std. Dev.	0.4	0.3	0.3	0.2	0.2	0.2	0.1	0.1	0.2	0.3	0.4	0.4
Rejected passages	Average	1.3	1.3	1.4	1.3	0.9	0.6	0.4	0.6	0.9	1.1	1.4	1.2
	Std. Dev.	0.2	0.2	0.2	0.1	0.2	0.1	0.1	0.1	0.1	0.2	0.3	0.3
Acceptable passages	Average	2.3	2.4	2.3	2.2	1.9	1.7	1.2	1.3	1.7	2.1	2.4	2.3
	Std. Dev.	0.3	0.4	0.2	0.2	0.2	0.2	0.0	0.1	0.2	0.3	0.3	0.4
Duration in days		Jan	Feb	Mar	Apr	May	Jun	Jul	Aug	Sep	Oct	Nov	Dec
All passages	Average	7.0	6.6	5.9	6.2	8.7	15.3	26.3	18.6	9.5	6.4	5.4	7.0
	Std. Dev.	1.3	1.2	1.0	0.8	1.5	3.5	7.0	3.9	1.8	1.2	1.0	2.2
Rejected passages	Average	8.5	8.3	7.8	8.8	11.7	17.2	26.3	18.9	12.8	9.8	8.1	8.9
	Std. Dev.	1.2	1.0	1.0	1.0	2.0	3.4	7.0	3.8	1.9	2.1	2.3	2.1
Acceptable passages	Average	4.8	4.6	4.9	5.1	5.9	6.5	8.9	8.2	6.5	5.3	4.6	4.7
	Std. Dev.	0.6	0.5	0.4	0.5	0.6	0.7	0.0	0.6	0.8	0.6	0.5	0.9
Distance Sailed Ratio		Jan	Feb	Mar	Apr	May	Jun	Jul	Aug	Sep	Oct	Nov	Dec
All passages	Average	1.6	1.5	1.4	1.4	1.7	2.7	4.4	3.1	1.7	1.3	1.3	1.6
	Std. Dev.	0.2	0.2	0.1	0.1	0.2	0.6	1.1	0.6	0.3	0.2	0.1	0.4
Rejected passages	Average	1.9	1.8	1.7	1.8	2.1	3.0	4.4	3.1	2.2	1.9	1.8	2.0
	Std. Dev.	0.2	0.2	0.2	0.2	0.3	0.6	1.1	0.6	0.3	0.3	0.4	0.4
Acceptable passages	Average	1.2	1.2	1.2	1.2	1.2	1.3	1.4	1.4	1.3	1.2	1.1	1.2
	Std. Dev.	0.1	0.1	0.1	0.0	0.1	0.1	0.0	0.1	0.1	0.0	0.0	0.1

Table 2
Dor to Pharos, an example of summarised environmental parameters.

Dor–Pharos													
Average of max wind speed in knots		Jan	Feb	Mar	Apr	May	Jun	Jul	Aug	Sep	Oct	Nov	Dec
All passages	Average	22.6	21.5	19.2	17.8	16.3	16.0	16.3	15.0	14.7	16.0	17.3	21.7
	Std. Dev.	2.7	3.0	1.6	1.6	0.9	0.9	1.2	0.5	1.2	1.5	1.9	2.9
Rejected passages	Average	26.4	24.9	22.4	19.8	17.2	16.4	16.3	15.0	15.1	18.6	23.5	25.9
	Std. Dev.	2.8	2.9	2.2	2.1	1.5	0.8	1.2	0.4	1.4	3.2	3.3	2.5
Acceptable passages	Average	17.4	17.1	17.3	16.8	15.6	14.3	12.1	13.3	14.2	15.0	15.4	16.7
	Std. Dev.	2.1	1.4	1.1	1.3	0.9	1.0	0.0	1.6	1.2	1.1	1.0	1.7
Average of max wave height in m		Jan	Feb	Mar	Apr	May	Jun	Jul	Aug	Sep	Oct	Nov	Dec
All passages	Average	2.7	2.5	1.9	1.5	1.2	1.4	1.5	1.3	1.3	1.4	1.7	2.6
	Std. Dev.	0.6	0.6	0.3	0.3	0.1	0.2	0.2	0.1	0.2	0.3	0.4	0.6
Rejected passages	Average	3.5	3.3	2.6	1.9	1.4	1.4	1.5	1.4	1.3	2.0	3.0	3.5
	Std. Dev.	0.7	0.7	0.5	0.5	0.3	0.2	0.2	0.1	0.2	0.7	0.8	0.6
Acceptable passages	Average	1.6	1.5	1.5	1.3	1.1	1.0	0.7	1.0	1.2	1.2	1.3	1.6
	Std. Dev.	0.3	0.2	0.2	0.2	0.1	0.2	0.0	0.1	0.2	0.2	0.2	0.4
Average wind speed in knots		Jan	Feb	Mar	Apr	May	Jun	Jul	Aug	Sep	Oct	Nov	Dec
All passages	Average	11.9	11.4	10.7	9.7	8.8	9.1	9.5	8.6	8.4	9.2	9.8	11.6
	Std. Dev.	1.3	1.6	0.7	1.0	0.5	0.5	0.7	0.4	0.5	1.0	1.1	1.2
Rejected passages	Average	13.2	12.4	11.9	10.0	8.9	9.3	9.5	8.6	8.4	9.4	11.9	13.0
	Std. Dev.	1.3	1.8	1.4	1.2	0.8	0.5	0.7	0.4	0.7	1.5	1.4	1.2
Acceptable passages	Average	9.9	10.0	10.0	9.5	8.8	8.2	6.8	8.4	8.3	8.9	9.3	9.9
	Std. Dev.	1.3	1.1	0.7	1.0	0.5	0.7	0.0	0.9	0.6	1.0	1.0	1.0
Average cloud cover in %		Jan	Feb	Mar	Apr	May	Jun	Jul	Aug	Sep	Oct	Nov	Dec
All passages	Average	46.3	41.7	33.4	27.4	20.5	10.1	11.8	13.3	13.4	25.4	39.1	44.9
	Std. Dev.	3.3	7.5	5.0	4.7	6.3	3.0	3.5	2.9	2.4	6.4	6.4	7.0
Rejected passages	Average	47.4	44.2	37.9	29.2	20.1	10.2	11.8	13.3	13.8	28.6	46.8	47.0
	Std. Dev.	4.2	6.6	7.3	5.2	6.6	2.9	3.5	2.9	3.4	9.3	7.8	7.3
Acceptable passages	Average	43.6	40.5	32.3	27.1	21.6	11.0	8.4	13.9	13.0	23.7	37.1	44.3
	Std. Dev.	5.8	10.8	7.2	6.2	7.7	5.6	0.0	3.9	4.6	6.7	6.4	8.9

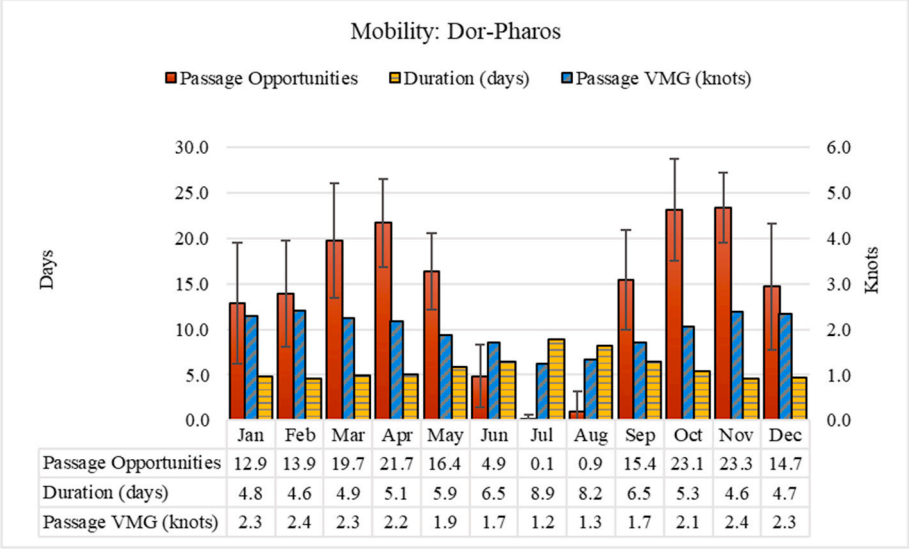

Fig. 9. Mobility for the passage from Dor to Pharos.

The synoptic systems that prevailed on the simulated departure date for each route segment are analysed on a monthly basis, and exemplified for the Dor to Pharos route segment in November (Fig. 13). The November average shows the high occurrence of the RST (14.3 days, blue bar), with 12.3 RST days providing opportunities for acceptable mobility (red bar). Similarly, the high-pressure system that is mostly associated with a RST to south (Saaroni et al., 2020), prevails on 9.5 days, with acceptable mobility on 7.5 days with the high-pressure system.

3.5. Sensitivity and comparative tests

As the criteria used to apply the human factor by distinguishing between 'acceptable' and 'rejected' passages represent a hypothetical ancient mariner (Section 2.6), it was deemed necessary to examine the effects of possible misjudgement of the criteria thresholds on the measured mobility. Two spot-checks were performed, one applying a lenient set of criteria all-at-once (representing a mariner taking more risks), and a second applying a strict set of criteria all-at-once (representing a mariner taking fewer risks). The test sets of criteria were arbitrarily set at plus or minus 1.5 standard deviations for each parameter to ensure applying more than a random change in the test criteria. The measured output of the tests was the change in the monthly patterns of mobility.

A more lenient mariner would clearly have higher mobility than a stricter one, as marginal sailings would be included in the set of

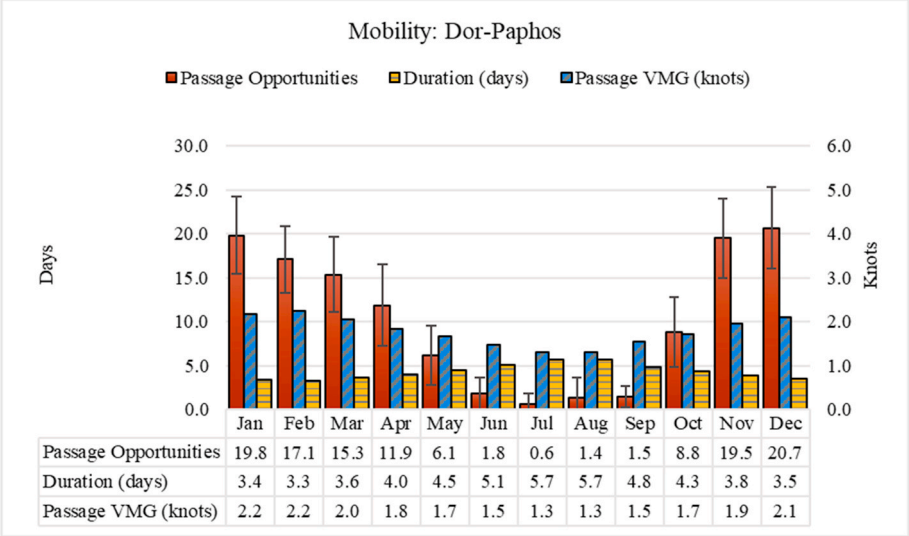

	Jan	Feb	Mar	Apr	May	Jun	Jul	Aug	Sep	Oct	Nov	Dec
Passage Opportunities	19.8	17.1	15.3	11.9	6.1	1.8	0.6	1.4	1.5	8.8	19.5	20.7
Duration (days)	3.4	3.3	3.6	4.0	4.5	5.1	5.7	5.7	4.8	4.3	3.8	3.5
Passage VMG (knots)	2.2	2.2	2.0	1.8	1.7	1.5	1.3	1.3	1.5	1.7	1.9	2.1

Fig. 10. Mobility for the passage from Dor to Paphos.

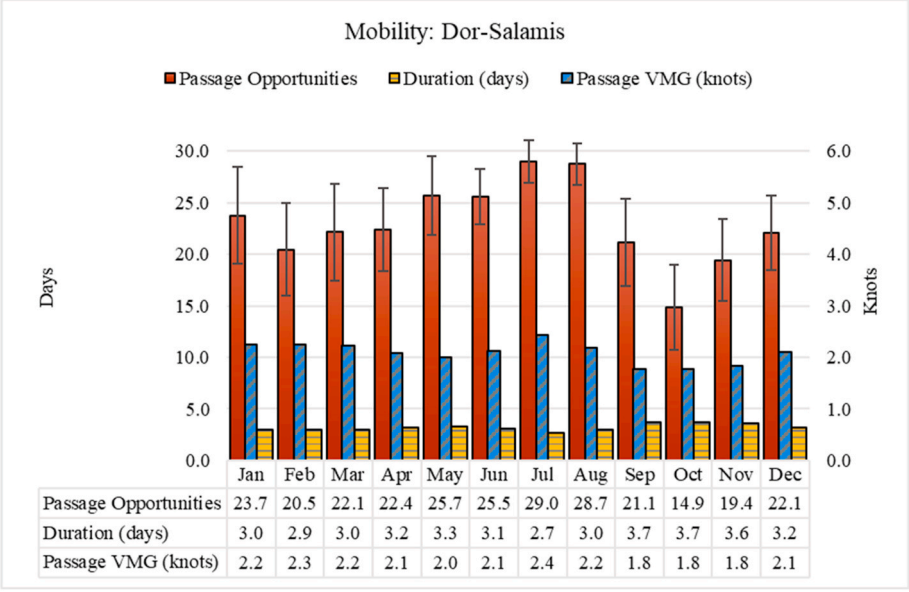

	Jan	Feb	Mar	Apr	May	Jun	Jul	Aug	Sep	Oct	Nov	Dec
Passage Opportunities	23.7	20.5	22.1	22.4	25.7	25.5	29.0	28.7	21.1	14.9	19.4	22.1
Duration (days)	3.0	2.9	3.0	3.2	3.3	3.1	2.7	3.0	3.7	3.7	3.6	3.2
Passage VMG (knots)	2.2	2.3	2.2	2.1	2.0	2.1	2.4	2.2	1.8	1.8	1.8	2.1

Fig. 11. Mobility for the passage from Dor to Salamis.

'acceptable' sailings, and vice-versa. Therefore, the objective of the tests was to establish, in passages considered contrary to the prevailing winds, whether the differences between a lenient and a strict mariner would change the general pattern of mobility on the passage. This applies particularly in the months of restricted mobility. The results are illustrated by plotting the proportional distribution of acceptable passage days over the months as a percentage of the annual total. Following are the results of the two examples considered representative of passages contrary to prevailing winds in the eastern Mediterranean. The Dor to Paphos passage (Fig. 14) indicates variations of 2%–3% from the baseline between April and September (see the table below the graph). For the Dor to Pharos route segment (Fig. 15), even smaller variations are evident.

The mobility of ships with higher levels of upwind capability were compared to that of the baseline-simulated ship. The comparative simulations were conducted on the Pharos to Rhodes route segment, which is considered representative of a passage contrary to the prevailing winds. The simulations were run for a vessel able of making good a course of 75° to the true wind, and for a second vessel able of making good a course of 70° to the true wind. The baseline ship for the simulations was able to make good 80° to the true wind (Section 2.5).

The results indicate a marginal increase in the mobility for the ship capable of 75° made good (Fig. 16). The ship capable of 70° made good demonstrated a more noticeable increase in upwind capabilities, particularly in the summer months, against the contrary Etesian winds. Mobility values reached about 12 days of 'acceptable' sailing opportunities in July and August versus only about 3 days for the baseline ship.

3.6. *Verification*

The ability of the method to identify windows-of-opportunity to sail to destinations contrary to the prevailing winds was verified in an actual sailing voyage by the *Ma'agan Mikhael II* from Dor (Israel) to Limassol (Cyprus). The method simulations, performed on weather forecast data during November 2018, showed two windows of opportunity, each with several good departure days during the second half of the month. The

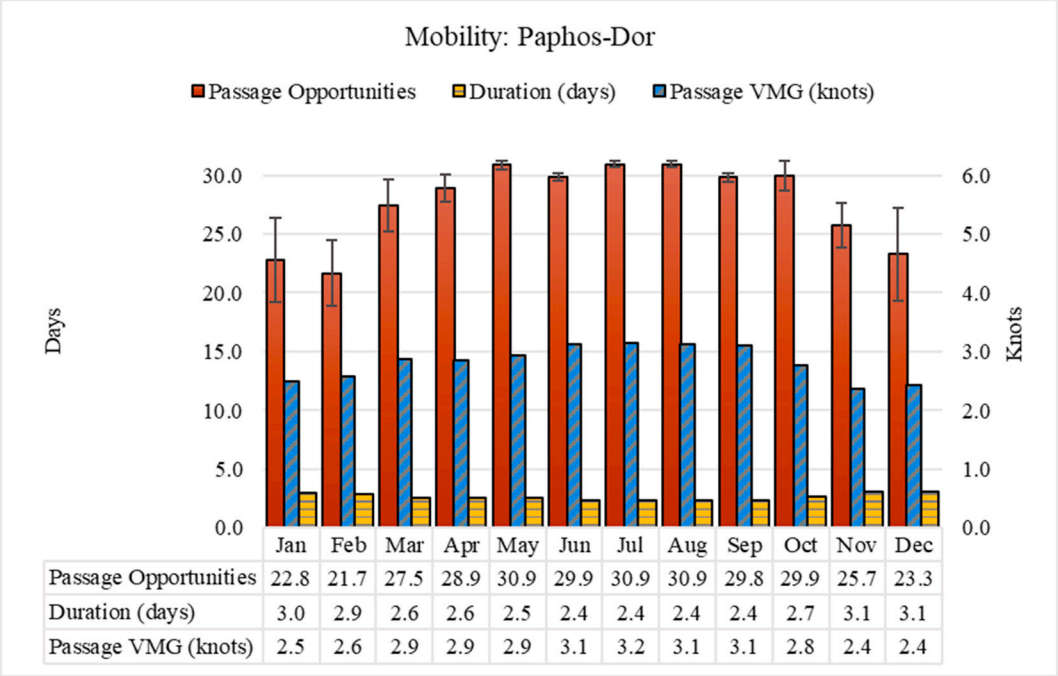

	Jan	Feb	Mar	Apr	May	Jun	Jul	Aug	Sep	Oct	Nov	Dec
Passage Opportunities	22.8	21.7	27.5	28.9	30.9	29.9	30.9	30.9	29.8	29.9	25.7	23.3
Duration (days)	3.0	2.9	2.6	2.6	2.5	2.4	2.4	2.4	2.4	2.7	3.1	3.1
Passage VMG (knots)	2.5	2.6	2.9	2.9	2.9	3.1	3.2	3.1	3.1	2.8	2.4	2.4

Fig. 12. Mobility for the passage from Paphos to Dor.

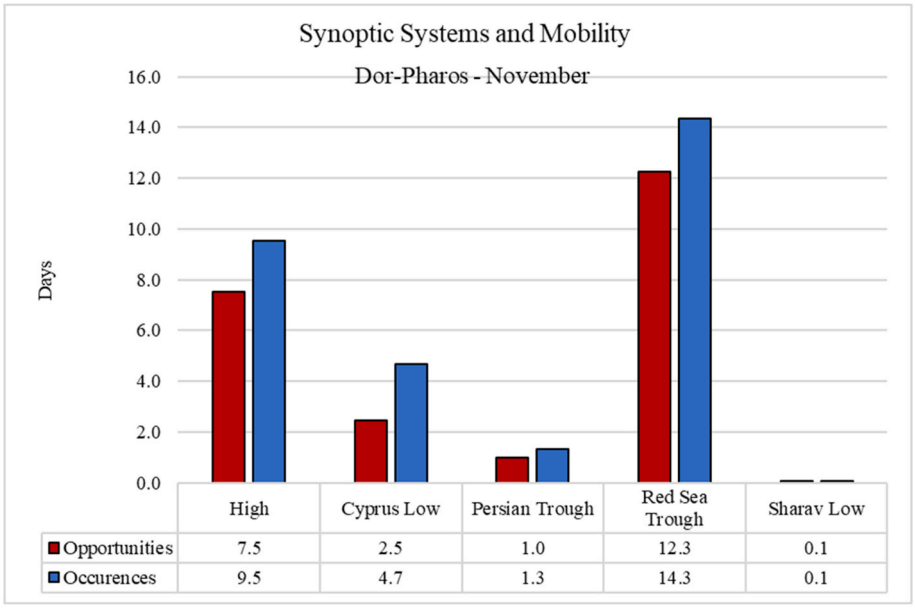

	High	Cyprus Low	Persian Trough	Red Sea Trough	Sharav Low
Opportunities	7.5	2.5	1.0	12.3	0.1
Occurences	9.5	4.7	1.3	14.3	0.1

Fig. 13. The number of opportunities for acceptable sailings that correspond with appearances of particular synoptic systems for the month of November on the Dor to Pharos passage.

second opportunity was taken, departing on 26th November. The simulation estimated a passage duration of 73 h, and the actual passage took 74 h, closely following the simulated route. This sailing voyage confirmed the feasibility of exploiting windows of opportunity with favourable winds necessary to conduct passages from the Levant contrary to prevailing winds by a 1st millennium BCE single-square-sail rig.

4. Summary and discussion

The method developed as a 'black box' integrates the environmental factors, the period ships' physical factors, and the ancient mariners' factors to establish measures of potential mobility. The sailing simulator is the component which combines the environmental factors with the ships' factors (without human factors) to generate the parameters of all sailing passages. The second component was the analysis of these multiple sailing results and the application of the human factors by means of criteria to divide the passages into sets of 'reasonable' for the mariners to have sailed and those 'unreasonable' to have sailed. The 'reasonable' set of passage provided the 'black box's' output of mobility measures, such as monthly count of passage opportunities, waiting time, passage VMG and duration.

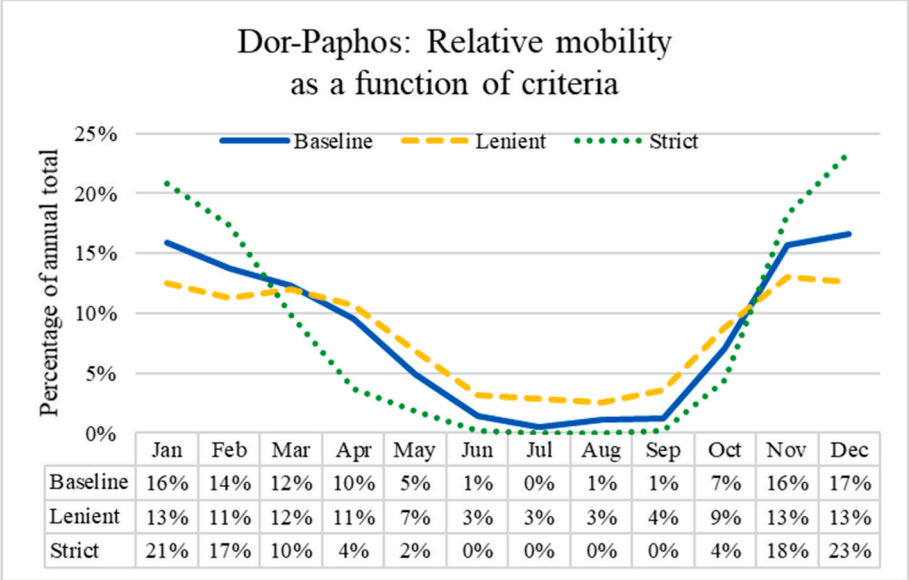

	Jan	Feb	Mar	Apr	May	Jun	Jul	Aug	Sep	Oct	Nov	Dec
Baseline	16%	14%	12%	10%	5%	1%	0%	1%	1%	7%	16%	17%
Lenient	13%	11%	12%	11%	7%	3%	3%	3%	4%	9%	13%	13%
Strict	21%	17%	10%	4%	2%	0%	0%	0%	0%	4%	18%	23%

Fig. 14. Criteria sensitivity test for the Dor to Paphos passage: relative mobility of criteria sets with values as percentage of annual total (%).

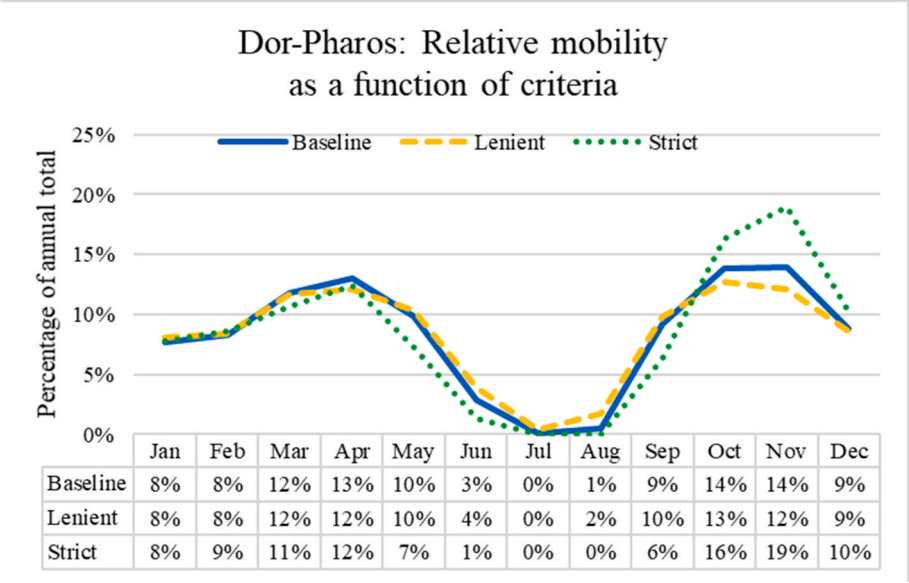

	Jan	Feb	Mar	Apr	May	Jun	Jul	Aug	Sep	Oct	Nov	Dec
Baseline	8%	8%	12%	13%	10%	3%	0%	1%	9%	14%	14%	9%
Lenient	8%	8%	12%	12%	10%	4%	0%	2%	10%	13%	12%	9%
Strict	8%	9%	11%	12%	7%	1%	0%	0%	6%	16%	19%	10%

Fig. 15. Criteria sensitivity test for the Dor to Pharos passage: relative mobility of three criteria sets with values as percentage of annual total (%).

4.1. Use of high-resolution climatological data

Using large data sets of wind and environment variables at high spatial and temporal resolutions, has demonstrated the feasibility and value of converting this data into finely detailed sailing data over a long enough study period to produce statistically significant results. The high spatio-temporal resolution used has exposed the opportunities for favourable winds resulting from the typical variabilities of the Mediterranean wind regimes. The multiple individual sailing simulations and their summaries provide insight regarding the seafaring issues that would have been encountered on each passage, and they also provide the ability to introduce the mariner's preferences and limitations.

4.2. The hypothetical mariner

Confidence in defining the hypothetical mariner's preferences and limitations was required, since these parameters influence the measures of mobility in the developed method. The sensitivity tests performed (Section 3.5) have shown that the differences in measured mobility are marginal for a wide spectrum of mariner thresholds; and the relative monthly patterns of mobility are hardly changed. This reflects the dominance of the environment on mobility.

4.3. Upwind sailing performance

This method requires that ship performance parameters be introduced as input. It has no direct ability to indicate what period ships' physical performance might have been. However, comparative simulations (Section 3.5) have indicated that overall mobility is affected more by the environment and by the mariners' limits than by the effective tacking angles of the ships.

The span of the scholarly discord on upwind sailing is broad (Section 1.1). However, the low sensitivities of mobility patterns to the ship performance inputs in Section 3.5, together with the dominance of the

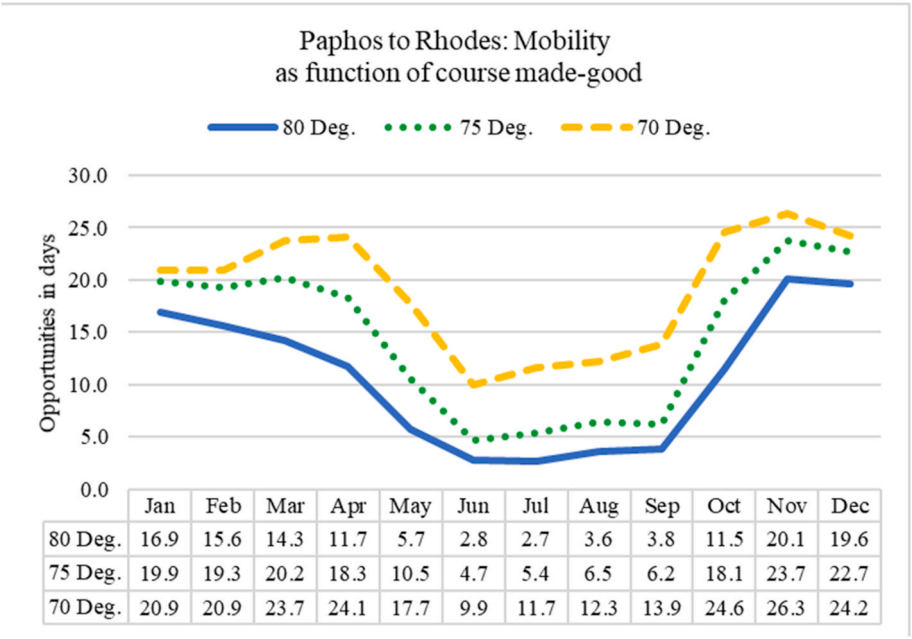

	Jan	Feb	Mar	Apr	May	Jun	Jul	Aug	Sep	Oct	Nov	Dec
80 Deg.	16.9	15.6	14.3	11.7	5.7	2.8	2.7	3.6	3.8	11.5	20.1	19.6
75 Deg.	19.9	19.3	20.2	18.3	10.5	4.7	5.4	6.5	6.2	18.1	23.7	22.7
70 Deg.	20.9	20.9	23.7	24.1	17.7	9.9	11.7	12.3	13.9	24.6	26.3	24.2

Fig. 16. Comparison of upwind performance on mobility with performance expressed by course made good to the true wind. Passage opportunities count on the Paphos to Rhodes passage, for the baseline ship (80° made-good) compared to ships with 75° and 70° made-good.

environmental and human factors, give confidence in the choice of simulating the middle-of-the-road ship (Section 1.1) which was based on the *Ma'agan Mikhael II*, adjusted to being able to maintain 80° made good to the true wind in all sea and wind conditions.

4.4. Case study observations

The objective of this work was to develop a method for measuring maritime mobility on direct sailing passages. The development testbed itself offered the opportunity to examine the issue of return routes from the Levant in light of contrary prevailing winds. Some contextual aspects of the outcome of the testbed application are briefly illustrated.

The results of the study have indicated that there are extremely limited opportunities to make return open water passages from the Levant in the months of June to September. This applies to all route options: direct via Paphos and Rhodes, northern routes via the coast of Anatolia or southern routes via Egypt and North Africa (Fig. 6). The transition seasons of March to May and October to November indicate a fair level of sailing opportunities (Figs. 9 and 10). The winter months also offer sailing opportunities for those that might have chosen to sail during winter. It can be concluded that the variabilities of the wind in seasons other than the summer, offer known instances of favourable winds in the opposite direction to that of the prevailing winds, and mariners would wait for these opportunities. This is reflected by the observations of Ibn Jubayr regarding departure from Acre (now Akko) (transl. Broadhurst, 1952, pp. 326–7):

> The blowing of the winds in these parts has a singular secret. It is that the east wind does not blow except in spring and autumn, and, save at those seasons, no voyages can be made and merchants will not bring their goods to Acre. The spring voyages begin in the middle of April, when the east wind blows until the end of May. […] The autumn voyages are from the middle of October, when the east wind (again) sets in motion […] for it blows for (only) fifteen days, more or less. There is no other suitable time, for the winds then vary, that from the west prevailing.

An additional testbed case study is the re-examination of a voyage from the literary record. Following Casson, the voyage of Mark the Deacon from Caesarea to Rhodes is known to have lasted 10 days in comparison with eastbound voyages lasting 5 days (Casson, 1995, pp. 289–291). Casson grouped this voyage with voyages assumed to have been sailed with unfavourable winds, leading to his conclusion that "… ancient vessels averaged from less than 2 to 2½ knots against the wind". Referring to Hill, we learn that Mark the Deacon departed Caesarea on 28 September (Hill, 1913, p. 42). Application of this method for examining the direct passage from Dor to Rhodes, indicates a sharp increase in opportunities for a passage with favourable winds in October, suggesting a passage duration of 9.5 days. Based on the results, it can be safely suggested that Mark the Deacon's ship anticipated the favourable winds for a westbound voyage in the last days of September, and did not sail with unfavourable winds.

4.5. Application

Sailing voyages in Antiquity were most likely a segmented hybrid affair. Direct sailing passages would be conducted when advantageous, and breeze-assisted coastal sailing might be conducted on various segments of the voyage when and if this offered advantages in mobility. The method presented in this paper is limited to the examination of direct sailing passages. The ability to examine the daily breeze-assisted runs of coastal sailing requires the development of a separate method with different algorithms, using much higher resolution of wind data capable of resolving local land and sea breezes. Such a tool is a work-in-progress, and once complete, the combination toolkit of the two methods will support comprehensive examinations of maritime mobility in Antiquity.

5. Conclusions

The innovative method for direct sailing passages addresses the issues of Mediterranean wind variability, while applying the human factor to quantitative measures of mobility. This has generated new yardsticks for mobility, including time spent waiting for favourable winds, and the probability of an acceptable passage for a particular route segment in a particular month.

When applied to a seafaring scenario, the method provides a much broader scope of insights into seafaring and mobility than previously available. The comprehensive toolkit, including the ability to examine coastal breeze-driven sailing, will provide even deeper insights into

seafaring options in a further study.

The method is versatile, and can be applied to different seafaring scenarios where knowledge gaps exist. The realistic measures of mobility can provide improved inputs to the cost factors in maritime connectivity network analyses.

Declaration of competing interest

The authors declare that they have no known competing financial interests or personal relationships that could have appeared to influence the work reported in this paper.

Acknowledgements

Many thanks to Yochai Palzur and 'Zulu' Shapiro, co-skippers of the *Ma'agan Mikhael II* replica ship, and to the rest of the crew for their assistance in dozens of hours of measurements and for sailing together from Israel to Cyprus and back during the winter, just to prove a point. We also thank John B. Tresman for English editing. Finally we thank the three anonymous reviewers for constructively adding valuable clarity and strength to this work.

References

Alberti, G., 2018. TRANSIT: a GIS toolbox for estimating the duration of ancient sail-powered navigation. Cartogr. Geogr. Inf. Sci. 45, 510–528. https://doi.org/10.1080/15230406.2017.1403376.

Alpert, P., Ziv, B., 1989. The Sharav cyclone: observations and some theoretical considerations. J. Geophys. Res. Atmos 94, 18495–18514.

Alpert, P., Osetinsky, I., Ziv, B., Shafir, H., 2004a. A new seasons definition based on classified daily synoptic systems: an example for the eastern Mediterranean. Int. J. Climatol. 24, 1013–1021. https://doi.org/10.1002/joc.1037.

Alpert, P., Osetinsky, I., Ziv, B., Shafir, H., 2004b. Semi-objective classification for daily synoptic systems: application to the eastern Mediterranean climate change. Int. J. Climatol. 24, 1001–1011. https://doi.org/10.1002/joc.1036.

Beresford, J., 2013. The Ancient Sailing Season. Brill, Leiden.

Berkovic, S., 2016. Synoptic classes as a predictor of hourly surface wind regimes: the case of the Central and Southern Israeli Coastal Plains. J. Appl. Meteorol. Climatol. 55, 1533–1547. https://doi.org/10.1175/JAMC-D-16-0093.1.

Berkovic, S., 2018. Wind regimes and their relation to synoptic variables using self-organizing maps. Adv. Sci. Res. 15, 1–9. https://doi.org/10.5194/asr-15-1-2018.

Bowditch, N., 2017. American Practical Navigator: an Epitome of Navigation and Nautical Astronomy, vol. 2. National Geospatial-Intelligence Agency, Springfield, Virginia.

Broadhurst, R., 1952. The Travels of Ibn Jubayr, Being the Chronicles of a Mediaeval Spanish Moor Concerning His Journey to the Egypt of Saladin, the Holy Cities of Arabia, Baghdad the City of the Caliphs, the Latin Kingdom of Jerusalem, and the Norman Kingdom of Sicily. Goodword, New Delhi.

Broodbank, C., 2013. The Making of the Middle Sea: A History of the Mediterranean from the Beginning to the Emergence of the Classical World. Thames & Hudson.

Cariolou, G.A., 1997. Kyrenia II: the return from Cyprus to Greece of the replica of a hellenic merchant ship. In: Swiny, S., Hohlfelder, R.L., Wylde Swiny, H. (Eds.), Res Maritimae: Cyprus and the Eastern Mediterranean from Prehistory to Late Antiquity. American Schools of Oriental Research, Massachusetts, pp. 83–97.

Casson, L., 1995. Ships and Seamanship in the Ancient World. The John Hopkins University Press, Baltimore and London.

Copernicus, C.D.S., 2019. ERA5 Hourly Data on Single Levels from 1979 to Present [WWW Document]. Copernicus. URL. https://cds.climate.copernicus.eu/cdsapp#!/dataset/reanalysis-era5-single-levels?tab=overview, 3.21.19.

Cvikel, D., Hillman, A., 2020. The construction of the Ma'agan Mikhael II ship. In: Under the Mediterranean: Studies in Maritime Archaeology. Sidestone Press, Leiden.

Davies, B., Bickler, S.H., 2013. Sailing the simulated seas: a new simulation for evaluating prehistoric seafaring. Across sp. Time. Pap. From 41st. Conf. Comput. Appl. Quant. Methods Archaeol. Perth 25–28. March 2013 215–223.

EC-Copernicus, 2016. Copernicus marine environment monitoring service [WWW Document]. URL. http://marine.copernicus.eu/, 6.21.19.

Gifford, E.W., Gifford, J., 1998. The sailing characteristics of Saxon ships. Archaeonautica 14, 177–184. https://doi.org/10.3406/nauti.1998.1202.

Harpaz, T., Ziv, B., Saaroni, H., Beja, E., 2014. Extreme summer temperatures in the East Mediterranean-dynamical analysis. Int. J. Climatol. 34, 849–862. https://doi.org/10.1002/joc.3727.

Hersbach, H., 2016. The ERA5 Atmospheric Reanalysis. Am. Geophys. Union, Fall Meet, 2016, Abstr. #NG33D-01.

Hill, G.F., 1913. The Life of Porphyry Bishop of Gaza by Mark the Deacon. Clarendon Press, Oxford.

Horden, P., Purcell, N., 2000. The Corrupting Sea: A Study of Mediterranean History. Blackwell Publishing Ltd, Oxford.

Kahanov, Y., Linder, E., 2004. Final Report. The Ma'agan Mikhael Ship. The Recovery of a 2400 Year-Old Merchantman, vol. II. Israel Exploration Society and University of Haifa, Jerusalem.

Kalnay, E., Kanamitsu, M., Kistler, R., Collins, W., Deaven, D., Gandin, L., Iredell, M., Saha, S., White, G., Woollen, J., Zhu, Y., Leetmaa, A., Reynolds, R., Chelliah, M., Ebisuzaki, W., Higgins, W., Joseph, D., 1996. The NCEP/NCAR 40-year reanalysis project. Bull. Am. Meteorol. Soc. 77, 437–471. https://doi.org/10.1175/1520-0477(1996)077<0437:TNYRP>2.0.CO, 2.

Katzev, M.L., 1990. An analysis of the experimental voyages of Kyrenia II. In: Tzalas, H.E. (Ed.), 2nd International Symposium on Ship Construction in Antiquity. Hellenic Institute for the Preservation of Nautical Tradition, Athens, pp. 245–256.

Kemp, P., 1976. The Oxford Companion to Ships and the Sea. Oxford University Press, London, New York, Melbourne.

Kistler, R., Kalnay, E., Collins, W., Saha, S., White, G., Woollen, J., Chelliah, M., Ebisuzaki, W., Kanamitsu, M., Kousky, V., 2001. The NCEP–NCAR 50-year reanalysis: monthly means CD-ROM and documentation. Bull. Am. Meteorol. Soc. 82, 247–268.

Klaic, Z.B., Pasaric, Z., Tudor, M., 2009. On the interplay between sea-land breezes and Etesian winds over the Adriatic. J. Mar. Syst. 78, S101–S118. https://doi.org/10.1016/j.jmarsys.2009.01.016.

Leidwanger, J., 2013. Modeling distance with time in ancient Mediterranean seafaring: a GIS application for the interpretation of maritime connectivity. J. Archaeol. Sci. 40, 3302–3308. https://doi.org/10.1016/j.jas.2013.03.016.

Linder, E., Kahanov, Y., 2003. Final Report. The Ma'agan Mikhael Ship. The Recovery of a 2400 Year-Old Merchantman, vol. I. Israel Exploration Society and University of Haifa, Jerusalem.

Lorenz, S.J., Kim, J.H., Rimbu, N., Schneider, R.R., Lohmann, G., 2006. Orbitally driven insolation forcing on Holocene climate trends: evidence from alkenone data and climate modeling. Paleoceanography 21, 1–14. https://doi.org/10.1029/2005PA001152.

McGrail, S., 2004. Boats of the World, from the Stone Age to Medieval Times. Oxford University Press, Oxford.

Meltimus, 2017. qtVlm: navigation and weather routing software [WWW Document]. meltimus.com. URL. https://www.meltemus.com/index.php/en/, 3.21.19.

Morton, J., 2001. The Role of the Physical Environment in Ancient Greek Seafaring. Brill, Leiden.

Murray, W.M., 1987. Do modern winds equal ancient winds? Mediterr. Hist. Rev. 2, 139–167.

Murray, W.M., 1993. Ancient sailing winds in the eastern mediterranean: the case for Cyprus. In: Proceedings of the International Symposium, Cyprus and the Sea. Nicosia. University of Cyprus, Nicosia, pp. 33–44.

Palmer, C., 2009. Windward sailing capabilities of ancient vessels. Int. J. Naut. Archaeol. 38, 314–330. https://doi.org/10.1111/j.1095-9270.2008.00208.x.

Pomey, P., Poveda, P., 2018. Gyptis: sailing replica of a 6th-century-BC archaic Greek sewn boat. Int. J. Naut. Archaeol. 47, 45–56. https://doi.org/10.1111/1095-9270.12294.

Pryor, J.H., 1988. Geography, Technology, and War: Studies in the Maritime History of the Mediterranean, 649–1571, Past and Present Publications. Cambridge University Press, Cambridge.

Pryor, J.H., 2014. The geographical conditions of galley navigation in the Mediterranean. In: Stuckey, J. (Ed.), The Eastern Mediterranean Frontier of Latin Christendom, pp. 17–38. https://doi.org/10.4324/9781315240169.

Rabaud, M., 2016. Optimal routing in sailing. In: Proceedings of the Conference Sports Physics. Palaiseau, France, pp. 1–6.

Rimbu, N., Lohmann, G., Kim, J.H., Arz, H.W., Schneider, R., 2003. Arctic/North Atlantic Oscillation signature in Holocene sea surface temperature trends as obtained from alkenone data. Geophys. Res. Lett. 30, 131–134. https://doi.org/10.1029/2002GL016570.

Saaroni, H., Bitan, A., Alpert, P., Ziv, B., 1996. Continental polar outbreaks into the levant and eastern mediterranean. Int. J. Climatol. 16, 1175–1191.

Saaroni, H., Ziv, B., Bitan, A., Alpert, P., 1998. Easterly wind storms over Israel. Theor. Appl. Climatol. 59, 61–77. https://doi.org/10.1007/s007040050013.

Saaroni, H., Ziv, B., 2000. Summer rain episodes in a Mediterranean climate, the case of Israel: climatological-dynamical analysis. Int. J. Climatol. 20, 191–209. https://doi.org/10.1002/(SICI)1097-0088(200002)20:2<191::AID-JOC464>3.0.CO;2-E.

Saaroni, H., Ziv, B., Osetinsky, I., Alpert, P., 2010. Factors governing the interannual variation and the long-term trend of the 850 hpa temperature over Israel. Q. J. R. Meteorol. Soc. 136, 305–318. https://doi.org/10.1002/qj.580.

Saaroni, H., Harpaz, T., Alpert, P., Ziv, B., 2020. Automatic identification and classification of the northern part of the Red Sea trough and its application for climatological analysis. Int. J. Climatol. 40, 3607–3622. https://doi.org/10.1002/joc.6416.

Safadi, C., Sturt, F., 2019. The warped sea of sailing: maritime topographies of space and time for the Bronze Age eastern Mediterranean. J. Archaeol. Sci. 103, 1–15. https://doi.org/10.1016/j.jas.2019.01.001.

Scheidel, W., Meeks, E., Weiland, J., 2012. ORBIS: the stanford geospatial network model of the roman world [WWW Document]. URL. http://orbis.stanford.edu/, 5.22.19.

Skibin, D., Hod, A., 1979. Subjective analysis of mesoscale flow patterns in northern Israel. J. Appl. Meteorol. 2.

Tsvieli, Y., Zangvil, A., 2005. Synoptic climatological analysis of "wet" and "dry" Red Sea Troughs over Israel. Int. J. Climatol. 25, 1997–2015. https://doi.org/10.1002/joc.1232.

UK Hydrographic Office, 2005. Mediterranean pilot volume V, ninth. In: The United Kingdom Hydrographic Office. Taunton, Somerset, UK.

Ulbrich, U., Lionello, P., Belušić, D., Jacobeit, J., Knippertz, P., Kuglitsch, F.G., Leckebusch, G.C., Luterbacher, J., Maugeri, M., Maheras, P., Nissen, K.M., Pavan, V.,

Pinto, J.G., Saaroni, H., Seubert, S., Toreti, A., Xoplaki, E., Ziv, B., 2012. Climate of the mediterranean: synoptic patterns, temperature, precipitation, winds, and their extremes. In: Lionello, P. (Ed.), The Climate of the Mediterranean Region. Elsevier, New York, pp. 301–346. https://doi.org/10.1016/B978-0-12-416042-2.00005-7.

Warnking, P., 2016. Roman trade routes in the mediterranean sea: modeling the routes and duration of ancient travel with modern offshore regatta software. In: Schäfer, C. (Ed.), Connecting the Ancient World: Mediterranean Shipping, Maritime Networks and Their Impact. Verlag Marie Leidorf GmbH, Rahden, Westf., pp. 45–90

Whitewright, J., 2011. The potential performance of ancient mediterranean sailing rigs. Int. J. Naut. Archaeol. 40, 2–17. https://doi.org/10.1111/j.1095-9270.2010.00276.x.

Whitewright, J., 2018. Sailing and Sailing Rigs in the Ancient Mediterranean: implications of continuity, variation and change in propulsion technology. Int. J. Naut. Archaeol. 47, 28–44. https://doi.org/10.1111/1095-9270.12278.

Ziv, B., Saaroni, H., Alpert, P., 2004. The factors governing the summer regime of the eastern Mediterranean. Int. J. Climatol. 24, 1859–1871. https://doi.org/10.1002/joc.1113.